# Macromolecules

Article

Thermoresponsive Membranes from Electrospun Mats with Switchable Wettability for Efficient Oil/Water Separations

Yan Liu,[†,‡] Sinem Tas,[‡] Kaihuan Zhang,[‡] Wiebe M. de Vos,[§] Jinghong Ma,*[,†] and G. Julius Vancso*[,‡]

[†]State Key Laboratory for Modification of Chemical Fibers and Polymer Materials, College of Materials Science and Engineering, Donghua University, 201620 Shanghai, P. R. China

[‡]Materials Science and Technology of Polymers, MESA+ Institute of Nanotechnology, and [§]Membrane Science and Technology, University of Twente, P.O. Box 217, 7500 AE Enschede, The Netherlands

Ⓢ *Supporting Information*
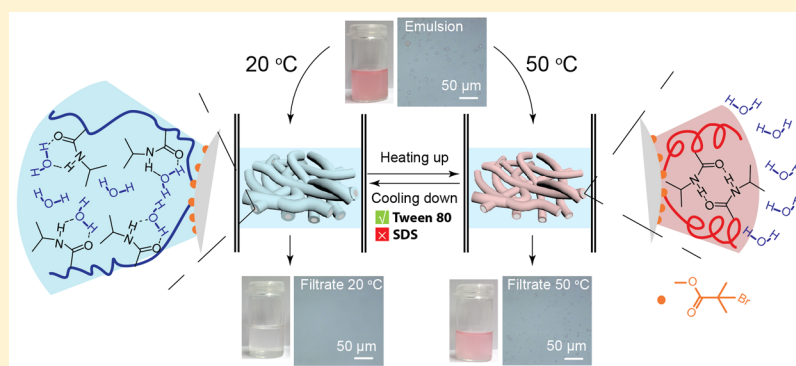
ABSTRACT: A simple and versatile method is described to obtain polycaprolactone (PCL) porous membranes, consisting of fibers prepared by electrospinning. The surface of the fibers is modified by grafting poly(*N*-isopropylacrylamide) (PNIPAM) brushes by surface-initiated atom-transfer radical polymerization (SI-ATRP). PCL mixtures, featuring Br end-functionalized and nonfunctionalized polymer, are used to enable SI-ATRP. Wettability at variable temperatures is governed by the lower critical solution temperature (LCST) of PNIPAM as contact angle and swelling ratio measurements demonstrate. Because of the PNIPAM LCST, the membranes show a variation of pore size with temperature, which is accompanied by flux changes of water permeating the membranes. Temperature gated separation is demonstrated using oil/water emulsions at 1 bar pressure. Typical separation efficiencies are 92% and 25% at 25 and 50 °C, respectively. Employment of anionic and neutral surfactants shows that the separation efficiency also depends on the interaction between the membranes and the emulsions.

INTRODUCTION

Materials decorated with stimuli-responsive polymer brushes[1] are playing an increasingly important role in various applications, such as drug delivery,[2] oil/water separation,[3] and tissue engineering.[4,5] Polymeric materials featuring engineered, responsive surfaces are ideal candidates for controlling and switching surface wettability, which provide scientifically exciting platforms for further research and also have a broad range of applications.[6−8] Wettability can be governed by the chemical composition and morphology of surfaces.[9,10] Hydrophobicity of a surface can be enhanced by altering the surface roughness of the substrates.[11−13] Hydrophilicity can be amplified e.g. by enhancing substrate porosity via capillary effects.[14,15] In addition, stimuli-responsive brushes can be grafted from (or to) both flat and porous substrates, which allows additional property steering.[16−20]

Oil/water separation is one of the technologically relevant applications for stimuli-responsive membrane constructs, addressed in this work. Such separations are, for example, relevant for the discharge of oily wastewater in industry and are utilized in frequent oil spill accidents that require thorough cleanup.[21] There are three types of separation materials that can be considered for such uses: encompassing "oil-removing" type platforms; "water-removing" type systems; and smart, controllable separation filters.[3] Compared with the other two types of materials, smart controllable separation materials have more advantages for facile fabrication of separation devices, including accelerated separation rate and reduced energy use. CO_2-responsive nanofibrous membranes with switchable oil/water wettability have, for example, been reported.[6]

Reversible switching between hydrophilicity and hydrophobicity has been demonstrated for oil/water separation by introducing PNIPAM brushes in porous membranes.[22] Dual-responsive materials have also been used for controllable oil/
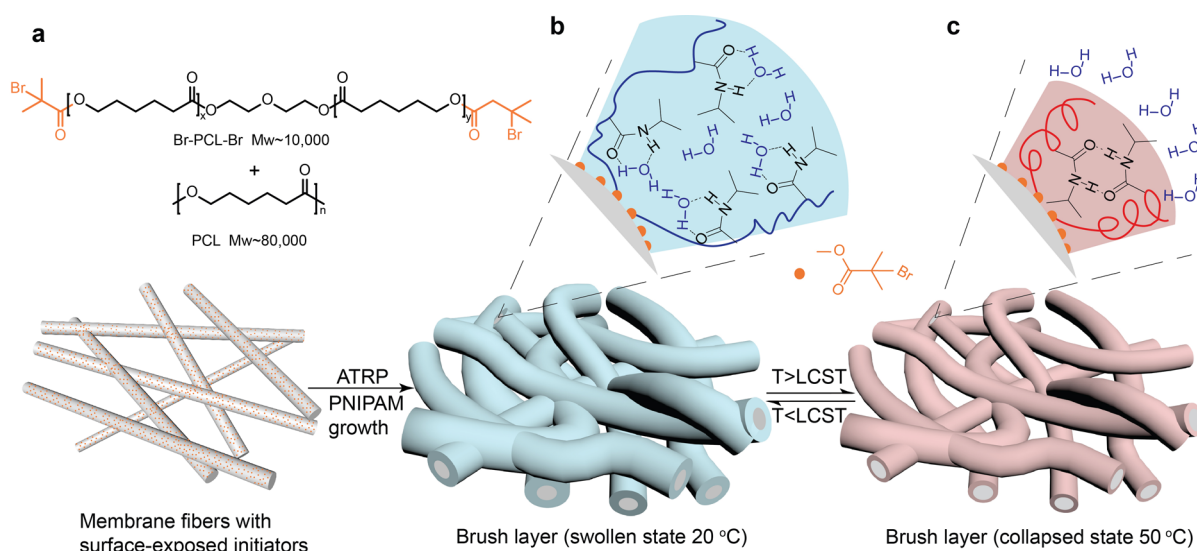
Figure 1. Preparation of thermoresponsive porous membranes. (a) Components of fibers and PCL porous membrane decorated with macroinitiators. (b) PCL-PNIPAM thermoresponsive porous membranes at swollen state. PNIPAM brush layers are swollen, and the membrane is hydrophilic at 20 °C (blue color). (c) PCL-PNIPAM thermoresponsive porous membrane at collapsed state. PNIPAM brush layers are collapsed, and the membrane is hydrophobic at 50 °C (red color).

water separation, which were obtained by photoinitiated free radical polymerization of (dimethylamino)ethyl methacrylate (DMAEMA).[3] Yet despite these attempts, "there is plenty of room" for new types of structures and constructs to be explored.

In this work, we report on the preparation of functional membranes featuring thermoresponsive PNIPAM brush grafted from porous electrospun mats by SI-ATRP. Figure 1 illustrates the process of preparation of these membrane platforms (thermoresponsive membranes). In Figure 1, the temperature responsive behavior is depicted in panels b and c. Below LCST, PNIPAM brushes will be swollen in water, while passing the LCST, at higher temperatures the brush coating will collapse, providing temperature responsivity.[23] The fiber surface in the hydrophilic, water-swollen state contributes to capillary wetting inside the membrane. The membrane decorated with macroinitiators without modification was hydrophobic and could not be permeated by water. However, the membrane grafted with PNIPAM brushes exhibited good water permeability.[4] Utilizing the difference of water penetration and permeability rates within the microporous membranes as a function of fiber surface wettability, we postulate that thermoresponsive membranes have application potential to control the flux of aqueous solution through designer membrane constructs. The flux experiments of aqueous penetrants were performed at different pressures to verify our hypothesis. As mentioned, the pore size is reduced below LCST as the PNIPAM brushes were swollen in membranes. After increasing the temperature to above LCST, the pore size changed to be larger as PNIPAM brushes were collapsed. This effect should contribute to the increase of water flux through the membrane. But the wettability of the membranes changed from hydrophilic to hydrophobic which is expected to decrease the flux of water. To confirm the effect of these two aspects, we checked the flux of water at 20 and 50 °C temperatures and from 1 to 3 bar pressures. From the results we can see that above LCST the flux of water is much larger than the value below LCST. All these experiments support our assumption that thermoresponsive membranes could be used

to control the flux of aqueous solutions. Based on the control of aqueous flux, thermoresponsive membranes were used in feasibility experiments to achieve the separation of oil-in-water emulsion.

■ EXPERIMENTAL SECTION

Materials. *N*-Isopropylacrylamide (NIPAM, Aldrich, 97%) was recrystallized twice from a toluene/hexane solution (50/50) and dried under vacuum for 48 h at room temperature. Copper(I) bromide (CuBr, Aldrich) was purified by stirring in glacial acid and washed with ethanol three times followed by drying under vacuum at room temperature. Polycaprolactone (PCL, average $M_n \sim$ 80000 g/mol), polycaprolactone (HO-PCL-OH, average $M_n \sim$ 10000 g/mol), α-bromoisobutyryl bromide (BIBB, 98%), triethylamine, copper(II) bromide (CuBr$_2$), 2,2′-bipyridine, *N,N,N′,N″,N″*-pentamethyl-diethylenetriamine (PMDETA), ethylenediaminetetraacetic acid tetrasodium salt dihydrate (EDTA, 99−102%), hexadecane, and methanol were purchased from Aldrich. Water was purified with a Milli-Q Advantage A10 purification system (Millipore, Billerica, MA).

Preparation of Nanofibers Featuring Br-Terminated Macroinitiators. The electrospun membrane fibers were spun from solutions of end-functionalized PCL macroinitiators and non-functionalized PCL. The macroinitiator Br-PCL-Br was synthesized by replacing terminal −OH groups of HO-PCL-OH ($M_n \sim$ 10000 g/mol) with BIBB. The synthetic process is described in the Supporting Information. The structure of the product is characterized by ^{1}H NMR (Figure S1 in the Supporting Information).[24] The macroinitiators were added into the electrospun precursor solution to prepare the porous membranes. The parameters of fabricating activated electrospun porous membranes are described in the Supporting Information.

Thermoresponsive Membranes Fabricated by SI-ATRP. Thermoresponsive membranes were fabricated by grafting PNIPAM brushes from the surface of nanofibers featuring Br-terminated species. The SI-ATRP was performed following standard experimental procedures. Before polymerization, all flasks were cleaned/washed using piranha solution. NIPAM (2 g, 17.4 mmol) and PMDETA (110 μL, 0.35 mmol) were added to a Milli-Q water (6.26 mL) and methanol (0.7 mL) mixture. The solution was flushed with argon for 30 min. Meanwhile, in another flask, CuBr (24.9 mg, 0.17 mmol) and CuBr$_2$ (3.9 mg, 0.017 mmol) were flushed with argon for 30 min. A 20 mL syringe was used to move the monomer and ligand solution
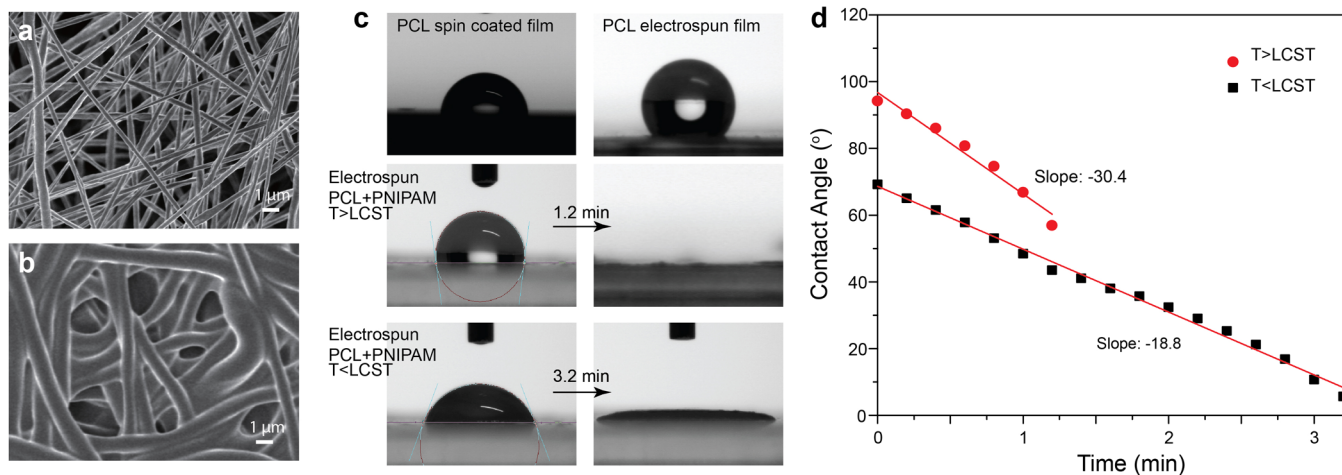
Figure 2. (a) Membranes decorated with macroinitiators. (b) Thermoresponsive porous membranes in the dry state. (c) Wettability of different membranes. (d) Time-dependent static contact angle of membranes below (rectangles) and above LCST (circles).

into the flask with CuBr and CuBr$_2$ for 30 min and bubbled with argon to form the organometallic complex. The solution obtained was then transferred into a flask degassed with argon containing the membrane decorated with Br-terminated macroinitiators. After 30 min, the reaction was terminated by adding water into the flask, and then the membranes were removed from the solution. Excess of water was used to remove any unreacted and not surface tethered substances. Finally, the membranes were rinsed in EDTA solution (0.1 M) to remove the copper catalyst and then dried with nitrogen gas for the water flux and oil/water separation measurements.

To illustrate the thermoresponsive property of PCL-PNIPAM membranes, the equilibrium swelling ratio (SR) as a function of temperature was studied gravimetrically. The samples were equilibrated in water over a temperature ranging from 20 to 50 °C. After wiping off the surface water with filter paper, the weight was measured (W_s). Then the weight values of corresponding dried membranes (W_d) were measured following an oven-drying step. The value of the SR is defined as the ratio of W_s and W_d.

Water Flux and Oil−Water Separation Measurements. To study switchable wettability of thermoresponsive membranes, water permeability experiments were performed using a dead-end filtration setup within the range of 1−3 bar. The dead-end filtration setup consisted of a 40 mL stirred filtration cell with compressed nitrogen as the driving force. The membranes were cut into a round shape with a diameter of 2.5 cm and subsequently placed in an Amicon type filter cell. For all experiments, the membranes were placed on top of a nonwoven fabric that acted as an additional mechanical support. Because the nonwoven fabric consists of relatively large voids and has a high permeability value (∼750000 L/m^2/h/bar), we assumed that it had no influence on the results of the permeability experiments.[25] To ensure a stable temperature, the cell was stored at a specific temperature at least for half an hour before the measurements.

Separation of oil/water emulsion was performed at two different temperatures 20 and 50 °C at 1 bar. Oil-in-water emulsions were prepared as follows: hexadecane (1 g) dyed with Oil Red O was added dropwise to 999 mL of water (with 10 mg/L Tween 80 or 2.5 g/L SDS as emulsifiers) under 14000 rpm for 10 min. As the hydrophobicity of the nonwoven fabric support has a negative influence on the separation, the support was removed in this experiment. The values of oil concentration in emulsion and filtrates after separation were determined by a UV−vis spectrophotometer (LAMBDA 850, PerkinElmer). The standard oil/water emulsion and the collected filtrates were sonicated for 0.5 h to obtain homogeneous solutions for UV−vis measurements. The separation efficiency value η was calculated based on the absorption data using Beer's law,[26] by the equation

$$\eta = \left(1 - \frac{C_r}{C_0}\right) \times 100\% = \left(1 - \frac{A_r}{A_0}\right) \times 100\% \tag{1}$$

where C_r represents the concentration of hexadecane in the filtrates, A_r stands for the absorption data of oil-dyed filtrates, C_0 is the initial concentration of hexadecane in the emulsion, and A_0 is the absorption data of oil-dyed emulsion. The absorption data were obtained at wavelength of 519 nm where the Oil Red O has a strong absorbance.

Chemical and Thermal Characterization. ^{1}H NMR spectra were collected in a Bruker Avance III spectrometer operated at 400 MHz. Samples were dissolved in CDCl$_3$, and the spectra were recorded at 295 K. Chemical shift values (δ) were expressed in parts per million with respect to the CDCl$_3$ signals. FTIR spectra (spectral resolution of 4 cm^{-1}, 256 scans) were obtained using a FTIR spectrometer (Nicolet 6700, Thermo Fisher). Differential scanning calorimetry (DSC) was performed using a PerkinElmer Pyris 1 DSC instrument (Waltham, MA). Wettability was measured with an OCA20 contact angle device (DataPhysics, Germany) at room temperature. A field-emission SEM (field emission JSM-633OF, JEOL Benelux) was used to obtain SEM images of membranes. The separation efficiencies at different temperatures were detected by a UV−vis spectrophotometer (LAMBDA 850, PerkinElmer).

■ RESULTS AND DISCUSSION

Structure of PCL-PNIPAM Thermoresponsive Porous Membranes. We first discuss the fabrication of brush-decorated PCL membrane mats. The membrane fibers were prepared by electrospinning as described in the Experimental Section. Because the alkyl bromide group (C−Br) is a polar (electronegative) species, the Br atom can acquire a partial negative charge. When spinning with the cathode positioned at the spinneret, the polymer fluids become positively charged at the surface. The positive charges will drive the C−Br groups to the surface by electrostatic attraction.[27] To verify the formation of PNIPAM brush layers, membranes decorated with macro-initiators and membranes featuring PNIPAM brush layers were characterized by FTIR and DSC. The FTIR spectra of membranes are shown in Figure S2. As can be seen from Figure S2, membranes decorated with macroinitiators showed the characteristic signal of carbonyl groups C═O from both end-functionalized PCL macroinitiators and nonfunctionalized PCL at 1730 cm^{-1} with a relatively strong absorbance, which indicates the presence of carbonyl groups in the polymer backbone.[28] The new peaks observed at 1645 and 1540 cm^{-1} in thermoresponsive porous membranes correspond to the
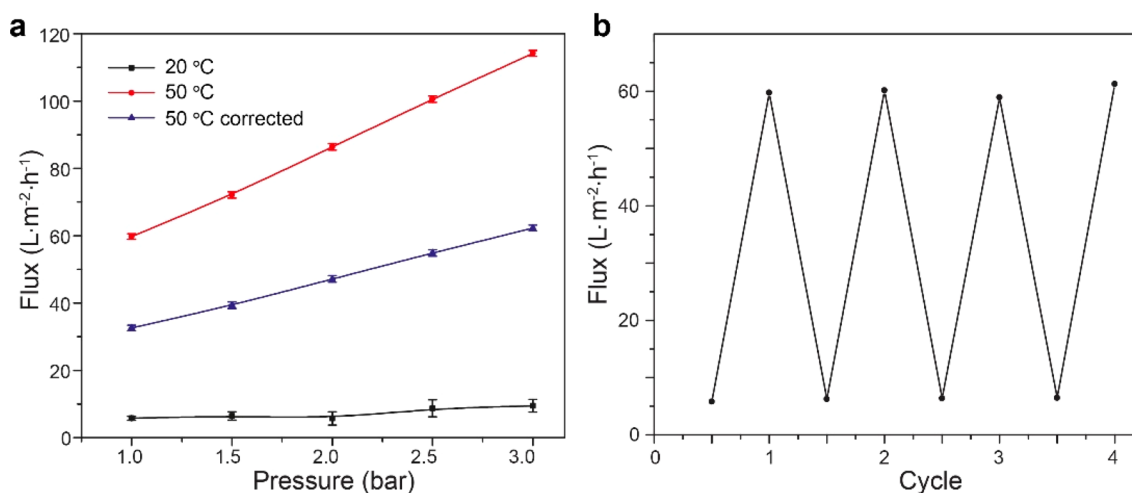
Figure 3. Flux below LCST and above LCST. (a) Flux at different temperature at the pressure in the range 1−3 bar. (b) Flux of PCL-PNIPAM thermoresponsive membranes at 1 bar switched between 20 and 50 °C (uncorrected for water viscosity variations). Half-integral cycles: T < LCST; integral cycles: T > LCST.

characteristic bonds for amide I and amide II, respectively.[29] Moreover, the broad peak appearing at 3400 cm^{-1} points to N−H bonds in PNIPAM polymer chains.[30] All results indicate the successful formation of PNIPAM polymer brushes on the surface of PCL fibers.

Thermal properties of the membranes were tested by DSC, and the results are shown in Figure S3. Membranes decorated with macroinitiators have a characteristic melting transition at 60 °C typical for PCL.[31] PCL-PNIPAM thermoresponsive porous membranes not only show a transition at 60 °C but also have a relatively weak step at 120 °C corresponding to the glass transition temperature of PNIPAM,[32] which also indicates the formation of polymer brushes.

In addition, to explore the LCST behavior, pieces of PCL-PNIPAM thermoresponsive membranes swollen in water (at 20 °C) were gradually heated to 55 °C. The values of the equilibrium swelling ratios at different temperatures are shown in Figure S4. The results illustrate that thermoresponsive membranes have a fast response and large deformation compared to the nonresponsive membranes without PNIPAM decoration.

Morphology of the Membranes by SEM. The typical morphologies of the membranes were characterized by high-resolution SEM. Representative results of the micrographs are shown in Figure 2. After grafting the PNIPAM brushes from the fibers, their average diameter increases significantly as compared to nanofibers without modification. Based on our previous work, the thickness of the PNIPAM brushes on a flat substrate in a dry state for the reaction conditions used is in the range of 250 nm as tested by atomic force microscopy (AFM) and ellipsometry.[33,34] This means that the anticipated diameter increase of the fibers in this work should be around 500 nm. As can be seen from Figure 2, the average diameter of the fibers increases by more than a factor 2 after growing PNIPAM brushes.

From Figure 2a,b, the average diameter of PCL nanofibers without modification is in the range of 300−350 nm, which can be determined as shown in Figure S5a. The average diameter of PCL-PNIPAM fibers is in the range of 800−850 nm; i.e., the increase of diameter will be around 500 nm as expected. Furthermore, we note that compared with macro-initiator decorated nanofibers prior to grafting, a pronounced

curvature and fiber bending appears following grafting. This interesting effect we tentatively attribute to axial buckling of the fibers due to the overgrown layer of the brush and the thus introduced axial stress. We note that this effect is explored in ongoing experiments.

Wettability of the Membranes. The wettability of membranes was characterized by contact angle measurements. Representative results are shown in Figure 2c. PCL spin-coated films have a contact angle of 83°, while electrospun membranes without PNIPAM brush modification were hydrophobic at room temperature with a contact angle of 131° as shown in Figure 2c.

The difference in contact angle values and its time dependence are related to the increased surface roughness of electrospun membranes at the nanoscale. After modification with PNIPAM brushes, water droplets were permeating into the membrane within 3.2 min at room temperature (<LCST) and showed a slow spreading. The main force for the absorption in this state is the hydrophilicity of PNIPAM layers and the capillary effect in the microporous membranes. However, when the temperature was increased to above LCST, the water droplet was permeating into the membrane completely in 1.2 min and spread very fast. As mentioned, wettability variations from hydrophobic to hydrophilic accompany the LCST. In addition, the pore size in membranes increased upon passing the transition. Here, we draw the conclusion that regarding variations of permeability, the effect of surface roughness change caused by the increases of pore size is stronger than the effect of the permeability reduced by the hydrophobic force. In addition, the rate of permeation above LCST is larger than below LCST, which can be represented by the slope of the contact angle in Figure 2d.

Water Permeability of Thermoresponsive Membranes. To study the switchable wettability of thermoresponsive membranes, water permeability experiments were performed at two different temperatures, below (20 °C) and above LCST (50 °C) in the pressure range 1−3 bar. Figure 3a shows the change in water fluxes at 20 and 50 °C as a function of pressure. A linear flux increase was observed with the pressure increase in all cases. We note that in the case of membrane compaction or rupture strong deviation from
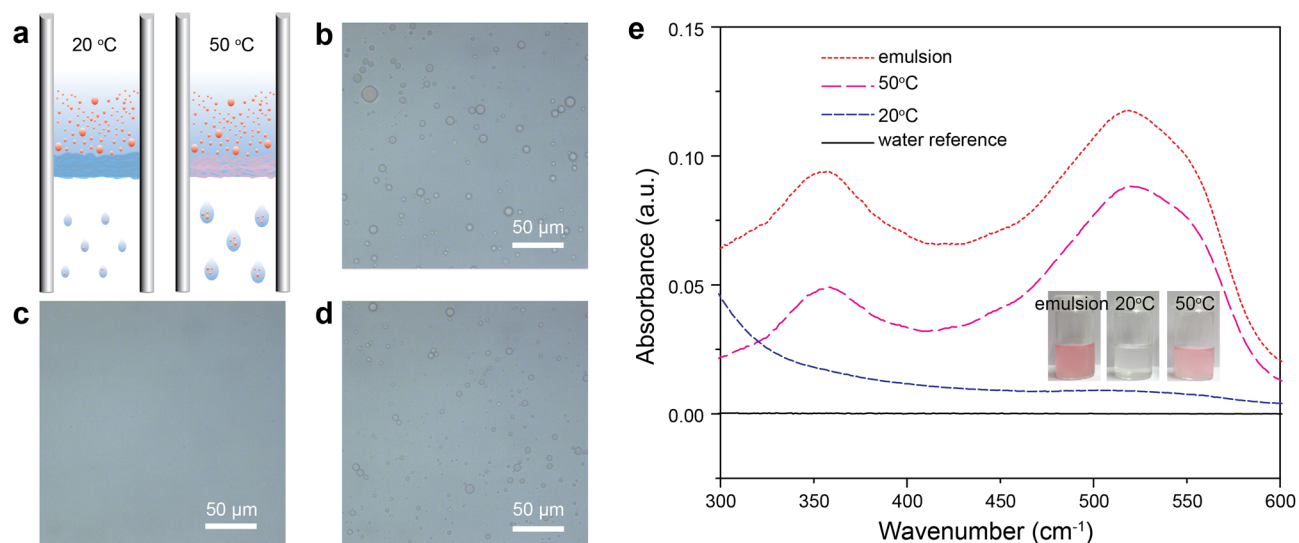
Figure 4. Tween 80 stabilized oil/water separation. (a) Scheme of thermoresponsive membranes at different temperature. (b−d) Optical images of the initial emulsion and filtrates at 20 and 50 °C. (e) UV−vis absorbance of the initial emulsion and filtrates at 20 and 50 °C.

linearity is expected. The linear increase observed demonstrates the mechanical stability of the membranes.

As it can be seen in Figure 3a, temperature variations had a considerable effect on the water flux. Generally, the rise in temperature increases permeation through the membrane due to a reduction in water viscosity. According to Poiseuille's law (eq 2)

$$J = \frac{\Delta p N \pi d^4}{128 \mu L} \tag{2}$$

where J is flux, N is the number of pores per square centimeter of the membrane, Δp is the pressure across the membrane, μ is the liquid viscosity, d is the diameter of the pore, and L is the length of the pore, the flux is reversely proportional to liquid viscosity.[35] The value of the viscosity of water is 1.0016 and 0.5465 mPa.s at 20 and 50 °C, respectively.[25] Therefore, for a true comparison of membrane permeability, the water fluxes were corrected by multiplying the flux values with the relative change in dynamic viscosity of water. The viscosity-corrected water flux values above LCST were clearly higher than the values below LCST.

The swollen/collapsed transition of the PNIPAM layer provides control of the pore size of the membranes. When the temperature is above LCST, PNIPAM polymer brushes collapse and yield enlarged membrane pores. Despite the hydrophobic surface, this was the main reason for higher water flux values as obtained for 50 °C compared with 20 °C, which is consistent with the conclusion obtained by contact angle measurements. Figure 3b shows the flux variation of a representative membrane at 20 and 50 °C observed over several cycles. The membrane exhibited identical water flux values for each temperature cycle within the experimental error, which indicated fully reversible thermoresponsive properties of the membrane.

Oil/Water Separation. Responsive membranes with switchable wettability are good candidates for the separation of oil/water emulsions.[22,36] To investigate the potential of our thermoresponsive PCL-PNIPAM nanofibrous membranes for separating oil/water emulsion, we performed dead-end filtration experiments under 1 bar of external pressure. Oil/

water (hexadecane 0.1 wt % in water) emulsions stabilized by nonionic (Tween 80, 10 mg/L) and ionic surfactant (SDS, 2.5 g/L) were prepared. The scheme of separation experiments at different temperatures is shown in Figure 4a. At 20 °C (<LCST), PNIPAM brushes are swollen and the membrane is hydrophilic; water could be absorbed into the membrane and pass through the membrane forced by hydrophilicity and capillary effect with few extremely small oil droplets permeating. However, when the temperature goes up to 50 °C (>LCST), PNIPAM brushes will be collapsed and the membrane will be hydrophobic; thus, larger oil droplets could also pass through the porous membrane due to the hydrophobicity of brushes and the increase of the pore size in the membrane.

For the filtration experiments, hexadecane was dyed by Oil Red O which could be detected by UV−vis spectroscopy. Figure 4e shows the UV−vis spectra of Oil Red O colored oil/water emulsion stabilized with Tween 80 and the spectra of the filtrates at 20 and 50 °C. Oil Red O has the first maximum absorbance at 360 nm and the second one at 519 nm. The PCL-PNIPAM membrane could separate 0.1 wt % oil-in-water emulsion at 20 °C with a high efficiency of 92%. However, the membrane exhibited a lower efficiency of 25% at 50 °C. Here, we need to mention that the critical micellar concentration (CMC) value of Tween 80 at temperature 20 and 50 °C was basically unchanged,[37] and the emulsions stabilized by nonionic surfactant were not expected to exhibit adhesion to the hydrophobic membrane fiber surface.[38]

Optical images of initial emulsions stabilized by Tween 80, filtrated at 20 and 50 °C, are shown in Figure 4b−d. The initial emulsion stabilized by Tween 80 has many oil droplets with diameter values within 1−10 μm (Figure 4b). After the separation, no visible oil droplets could be found in the filtered section at 20 °C (Figure 4c), but many small oil droplets with diameter in the range 1−5 μm could be observed at 50 °C (Figure 4d).

We also performed separation experiments for SDS stabilized oil/water emulsion at 20 and 50 °C. The UV−vis spectra of the emulsion and the filtrates at 20 and 50 °C are shown in Figure S6. Compared to the emulsion stabilized by nonionic Tween 80, high separation efficiencies of 99% and

98% were achieved at 20 and 50 °C, respectively. The difference in separation efficiency of SDS-stabilized emulsion between 20 and 50 °C was obviously substantially reduced as compared with the Tween 80-stabilized emulsion.

Two reasons might be considered to explain these results. One is that the LCST of PNIPAM brushes is shifted due to the added charge by SDS attached to the polymer. We note that the effect of SDS on the phase transition of PNIPAM dissolved in water, or in microgels, has been described.[39−42] The so-called "necklace model" and the "rod model" were proposed to describe these PNIPAM SDS complexes.[43,44] However, only few studies on the effect of SDS on tethered PNIPAM brushes were published.[45] In this work, the effect of SDS on tethered PNIPAM brushes is important as the high concentration of SDS used to prepare the emulsion may shift the LSCT or even make it disappear. The other possibility to explain the results could be that the increase of temperature enhanced the adhesion interaction between oil droplets and PNIPAM brushes at 50 °C, as the strength of the adhesion of SDS stabilized oil/water emulsion is temperature dependent.[46,47] Additionally, the oil droplets absorbed in the membrane can further enhance the adhesion interaction.

This observation is interesting as it demonstrates an alternative switching/responsivity mechanism for our PNIPAM functionalized membranes. At higher temperature (>LCST) and without surfactants the PNIPAM chains would be collapsed allowing for a membrane with a high flux an thus productivity. However, if the water that is treated becomes polluted with an emulsion (and thus surfactant), the PNIPAM chains would swell to close off the pores, leading to a rejection of the oil droplets. It would thus be possible to design a membrane that would sense and automatically adapt to the presence of an emulsion (stabilized by SDS) in the feed stream.

It is important to note that in many oil−water separations salt ions would also be expected to be present. For the nonionic surfactant, this will not change the observed separation behavior, but for the anionically stabilized emulsions, the presence of salt is expected to lead to increased membrane fouling, as the repulsion between oil droplets would decrease.[47] However, if the membrane would become fouled, the responsive nature of the membrane would again be of benefit. Responsive membranes can be more easily cleaned than traditional membranes, as a quick switch from a hydrophobic to a hydrophilic state, or vice versa, can lead to detachment of attached foulants.[48] Moreover, by opening the pores of the membrane, higher fluxes and thus higher shear forces can be used for improved physical cleaning.

CONCLUSIONS

Thermoresponsive membranes with switchable wettability were fabricated by electrospinning and SI-ATRP. Membranes decorated with Br-terminated macroinitiators were prepared first by electrospinning. Then the nanofibers were modified by grafting PNIPAM brushes from their surface. The structure of PCL−PNIAPM thermoresponsive membranes was characterized by FTIR and DSC. The results proved the successful modification of the PCL fibers with PNIPAM brushes. This was also supported by the large swelling ratio (SR ∼ 9) of the membranes. The morphology of the membranes was characterized by SEM. The results showed nanofibers in the nonfunctionalized membrane, with an average diameter in the range 300−350 nm, while after the modification, the diameter

increased to 800−850 nm. This finding provided yet another additional evidence proving the presence of the PNIPAM brushes at the fiber surface. The wettability of membranes was characterized by contact angle measurements, and the results illustrated that thermoresponsive membranes had different water absorption rates at 20 and 50 °C. The water permeability of thermoresponsive membranes was studied, and the results illustrated that thermoresponsive membranes were stable under 1−3 bar and could be used to control the flux of aqueous solutions by variations of the temperature. As an application with practical relevance, we studied the separation of oil/water emulsions. We found that the oil/water separation efficiency at different temperature will be affected not only by the properties of the membranes but also by the properties of the surfactant. Oil/water separation results showed that thermoresponsive membranes were able to separate the oil/water emulsion stabilized by Tween 80 at 25 °C with a high separation efficiency of 92% and with the substantially lower separation efficiency of 25% at 50 °C. However, the difference of separation efficiency at 20 and 50 °C was reduced for SDS stabilized emulsions. The low-cost thermoresponsive membrane described has great potential in industrial applications that require switchable separation.

ASSOCIATED CONTENT

Ⓢ Supporting Information

The Supporting Information is available free of charge on the ACS Publications website at DOI: 10.1021/acs.macromol.8b01853.

> FTIR measurement, DSC trace, volume phase transition, distribution of fibers diameter, separation results of SDS stabilized oil/water emulsion, and XPS spectrum (PDF)

AUTHOR INFORMATION

Corresponding Authors

*E-mail: mjh68@dhu.edu.cn (J.M.).
*E-mail: g.j.vancso@utwente.nl (G.J.V.).

ORCID Ⓘ

Yan Liu: 0000-0001-7933-7957
Kaihuan Zhang: 0000-0002-7353-4180
Wiebe M. de Vos: 0000-0002-0133-1931
G. Julius Vancso: 0000-0003-4718-0507

Present Address

K.Z.: Laboratory for Surface Science and Technology, Department of Materials, ETH Zürich, Vladimir-Prelog-Weg 1-5/10, 8093 Zürich, Switzerland.

Notes

The authors declare no competing financial interest.

REFERENCES

(1) Zoppe, J. O.; Ataman, N. C.; Mocny, P.; Wang, J.; Moraes, J.; Klok, H.-A. Surface-initiated controlled radical polymerization: state-of-the-art, opportunities, and challenges in surface and interface engineering with polymer brushes. *Chem. Rev.* **2017**, *117*, 1105−1318.

(2) Bajpai, A. K.; Shukla, S. K.; Bhanu, S.; Kankane, S. Responsive polymers in controlled drug delivery. *Prog. Polym. Sci.* **2008**, *33*, 1088−1118.

(3) Cao, Y.; Liu, N.; Fu, C.; Li, K.; Tao, L.; Feng, L.; Wei, Y. Thermo and pH dual-responsive materials for controllable oil/water separation. *ACS Appl. Mater. Interfaces* **2014**, *6*, 2026−2030.

(4) Gunnewiek, M. K.; Di Luca, A.; Bollemaat, H. Z.; van Blitterswijk, C. A.; Vancso, G. J.; Moroni, L.; Benetti, E. M. Creeping Proteins in Microporous Structures: Polymer Brush-Assisted Fabrication of 3D Gradients for Tissue Engineering. *Adv. Healthcare Mater.* **2015**, *4*, 1169−1174.

(5) Stuart, M. A. C.; Huck, W. T.; Genzer, J.; Müller, M.; Ober, C.; Stamm, M.; Sukhorukov, G. B.; Szleifer, I.; Tsukruk, V. V.; Urban, M.; et al. Emerging applications of stimuli-responsive polymer materials. *Nat. Mater.* **2010**, *9*, 101.

(6) Che, H.; Huo, M.; Peng, L.; Fang, T.; Liu, N.; Feng, L.; Wei, Y.; Yuan, J. CO_2-Responsive Nanofibrous Membranes with Switchable Oil/Water Wettability. *Angew. Chem., Int. Ed.* **2015**, *54*, 8934−8938.

(7) Yao, X.; Song, Y.; Jiang, L. Applications of bio-inspired special wettable surfaces. *Adv. Mater.* **2011**, *23*, 719−734.

(8) Wang, X.; Yu, J.; Sun, G.; Ding, B. Electrospun nanofibrous materials: a versatile medium for effective oil/water separation. *Mater. Today* **2016**, *19*, 403−414.

(9) Zhang, J.; Han, Y. A Topography/Chemical Composition Gradient Polystyrene Surface: Toward the Investigation of the Relationship between Surface Wettability and Surface Structure and Chemical Composition. *Langmuir* **2008**, *24*, 796−801.

(10) Zhang, P.; Wang, S.; Wang, S.; Jiang, L. Superwetting surfaces under different media: Effects of surface topography on wettability. *Small* **2015**, *11*, 1939−1946.

(11) Feng, L.; Song, Y.; Zhai, J.; Liu, B.; Xu, J.; Jiang, L.; Zhu, D. Creation of a superhydrophobic surface from an amphiphilic polymer. *Angew. Chem.* **2003**, *115*, 824−826.

(12) Li, H.; Wang, X.; Song, Y.; Liu, Y.; Li, Q.; Jiang, L.; Zhu, D. Super-"Amphiphobic" Aligned Carbon Nanotube Films. *Angew. Chem., Int. Ed.* **2001**, *40*, 1743−1746.

(13) Bocquet, L.; Lauga, E. A smooth future? *Nat. Mater.* **2011**, *10*, 334−337.

(14) Adera, S.; Raj, R.; Enright, R.; Wang, E. N. Non-wetting droplets on hot superhydrophilic surfaces. *Nat. Commun.* **2013**, *4*, 2518.

(15) Yu, X.; Wang, Z.; Jiang, Y.; Shi, F.; Zhang, X. Reversible pH-Responsive Surface: From Superhydrophobicity to Superhydrophilicity. *Adv. Mater.* **2005**, *17*, 1289−1293.

(16) Costantini, F.; Benetti, E. M.; Tiggelaar, R. M.; Gardeniers, H. J.; Reinhoudt, D. N.; Huskens, J.; Vancso, G. J.; Verboom, W. A Brush-Gel/Metal-Nanoparticle Hybrid Film as an Efficient Supported Catalyst in Glass Microreactors. *Chem. - Eur. J.* **2010**, *16*, 12406−12411.

(17) Sui, X.; Zapotoczny, S.; Benetti, E. M.; Memesa, M.; Hempenius, M. A.; Vancso, G. J. Grafting mixed responsive brushes of poly(N-isopropylacrylamide) and poly(methacrylic acid) from gold by selective initiation. *Polym. Chem.* **2011**, *2*, 879−884.

(18) Yu, Y.; Kieviet, B. D.; Liu, F.; Siretanu, I.; Kutnyanszky, E.; Vancso, G. J.; de Beer, S. Stretching of collapsed polymers causes an enhanced dissipative response of PNIPAM brushes near their LCST. *Soft Matter* **2015**, *11*, 8508−8516.

(19) Ramakrishna, S. N.; Cirelli, M.; Divandari, M.; Benetti, E. M. Effects of Lateral Deformation by Thermoresponsive Polymer Brushes on the Measured Friction Forces. *Langmuir* **2017**, *33*, 4164−4171.

(20) Yu, Y.; de la Cruz, R. A. L.; Kieviet, B. D.; Gojzewski, H.; Pons, A.; Vancso, G. J.; de Beer, S. Pick up, move and release of nanoparticles utilizing co-non-solvency of PNIPAM brushes. *Nanoscale* **2017**, *9*, 1670−1675.

(21) Shannon, M. A.; Bohn, P. W.; Elimelech, M.; Georgiadis, J. G.; Mariñas, B. J.; Mayes, A. M. Science and technology for water purification in the coming decades. *Nature* **2010**, *452*, 337−346.

(22) Ou, R.; Wei, J.; Jiang, L.; Simon, G. P.; Wang, H. Robust Thermoresponsive Polymer Composite Membrane with Switchable Superhydrophilicity and Superhydrophobicity for Efficient Oil−Water Separation. *Environ. Sci. Technol.* **2016**, *50*, 906−914.

(23) Yamada, N.; Okano, T.; Sakai, H.; Karikusa, F.; Sawasaki, Y.; Sakurai, Y. Thermo-responsive polymeric surfaces; control of attachment and detachment of cultured cells. *Makromol. Chem., Rapid Commun.* **1990**, *11*, 571−576.

(24) Harrison, R. H.; Steele, J. A. M.; Chapman, R.; Gormley, A. J.; Chow, L. W.; Mahat, M. M.; Podhorska, L.; Palgrave, R. G.; Payne, D. J.; Hettiaratchy, S. P.; Dunlop, I. E.; Stevens, M. M. Modular and Versatile Spatial Functionalization of Tissue Engineering Scaffolds through Fiber-Initiated Controlled Radical Polymerization. *Adv. Funct. Mater.* **2015**, *25*, 5748−5757.

(25) Cetintas, M.; De Grooth, J.; Hofman, A. H.; Van der Kooij, H. M.; Loos, K.; De Vos, W. M.; Kamperman, M. Free-standing thermoresponsive nanoporous membranes from high molecular weight PS-PNIPAM block copolymers synthesized via RAFT polymerization. *Polym. Chem.* **2017**, *8*, 2235−2243.

(26) Rohrbach, K.; Li, Y.; Zhu, H.; Liu, Z.; Dai, J.; Andreasen, J.; Hu, L. A cellulose based hydrophilic, oleophobic hydrated filter for water/oil separation. *Chem. Commun.* **2014**, *50*, 13296−13299.

(27) Fu, G. D.; Lei, J. Y.; Yao, C.; Li, X. S.; Yao, F.; Nie, S. Z.; Kang, E. T.; Neoh, K. G. Core−Sheath Nanofibers from Combined Atom Transfer Radical Polymerization and Electrospinning. *Macromolecules* **2008**, *41*, 6854−6858.

(28) Yuan, S.; Xiong, G.; Wang, X.; Zhang, S.; Choong, C. Surface modification of polycaprolactone substrates using collagen-conjugated poly (methacrylic acid) brushes for the regulation of cell proliferation and endothelialisation. *J. Mater. Chem.* **2012**, *22*, 13039−13049.

(29) Liu, Y.; Zhang, K.; Ma, J.; Vancso, G. J. Thermoresponsive Semi-IPN Hydrogel Microfibers from Continuous Fluidic Processing with High Elasticity and Fast Actuation. *ACS Appl. Mater. Interfaces* **2017**, *9*, 901−908.

(30) Zhu, D.; Lu, M.; Guo, J.; Liang, L.; Lan, Y. Effect of adamantyl methacrylate on the thermal and mechanical properties of thermosensitive poly (N-isopropylacrylamide) hydrogels. *J. Appl. Polym. Sci.* **2012**, *124*, 155−163.

(31) Kweon, H.; Yoo, M. K.; Park, I. K.; Kim, T. H.; Lee, H. C.; Lee, H. S.; Oh, J. S.; Akaike, T.; Cho, C. S. A novel degradable polycaprolactone networks for tissue engineering. *Biomaterials* **2003**, *24*, 801−808.

(32) Li, S.; Su, Y.; Dan, M.; Zhang, W. Thermo-responsive ABA triblock copolymer of PVEA-b-PNIPAM-b-PVEA showing solvent-tunable LCST in a methanol−water mixture. *Polym. Chem.* **2014**, *5*, 1219−1228.

(33) Kaholek, M.; Lee, W.-K.; Ahn, S.-J.; Ma, H.; Caster, K. C.; LaMattina, B.; Zauscher, S. Stimulus-Responsive Poly(N-isopropylacrylamide) Brushes and Nanopatterns Prepared by Surface-Initiated Polymerization. *Chem. Mater.* **2004**, *16*, 3688−3696.

(34) Sui, X.; Chen, Q.; Hempenius, M. A.; Vancso, G. J. Probing the Collapse Dynamics of Poly (N-isopropylacrylamide) Brushes by AFM: Effects of Co-nonsolvency and Grafting Densities. *Small* **2011**, *7*, 1440−1447.

(35) Baker, R. W. *Membrane technology*; Wiley Online Library: 2000.

(36) Kota, A. K.; Kwon, G.; Choi, W.; Mabry, J. M.; Tuteja, A. Hygro-responsive membranes for effective oil−water separation. *Nat. Commun.* **2012**, *3*, 1025.

(37) Mahmood, M. E.; Al-Koofee, D. A. Effect of temperature changes on critical micelle concentration for tween series surfactant. *Global J. Sci. Front Res. Chem.* **2013**, *13*, 1−8.

(38) Poulin, P.; Bibette, J. Adhesion between pure and mixed surfactant layers. *Langmuir* **1999**, *15*, 4731−4739.

(39) Wu, C.; Zhou, S. Effects of surfactants on the phase transition of poly (N-isopropylacrylamide) in water. *J. Polym. Sci., Part B: Polym. Phys.* **1996**, *34*, 1597−1604.

(40) Jean, B.; Lee, L.-T. Effects of sodium dodecyl sulfate on poly(N-isopropylacrylamide) adsorption at the air−water interface

above the lower critical solubility temperature. *Colloid Polym. Sci.* **2002**, *280*, 689−694.

(41) Jean, B.; Lee, L.-T. Noninteracting versus Interacting Poly(N-isopropylacrylamide)-Surfactant Mixtures at the Air-Water Interface. *J. Phys. Chem. B* **2005**, *109*, 5162−5167.

(42) Chen, J.; Gong, X.; Yang, H.; Yao, Y.; Xu, M.; Chen, Q.; Cheng, R. NMR study on the effects of sodium n-dodecyl sulfate on the coil-to-globule transition of poly (N-isopropylacrylamide) in aqueous solutions. *Macromolecules* **2011**, *44*, 6227−6231.

(43) Kokufuta, E.; Zhang, Y. Q.; Tanaka, T.; Mamada, A. Effects of surfactants on the phase transition of poly(N-isopropylacrylamide) gel. *Macromolecules* **1993**, *26*, 1053−1059.

(44) Lee, L.-T.; Cabane, B. Effects of Surfactants on Thermally Collapsed Poly(N-isopropylacrylamide) Macromolecules. *Macromolecules* **1997**, *30*, 6559−6566.

(45) Zhu, P. W. Effects of Sodium Dodecyl Sulfate on Structures of Poly(N-isopropylacrylamide) at the Particle Surface. *J. Phys. Chem. B* **2015**, *119*, 359−371.

(46) Bibette, J.; Mason, T.; Gang, H.; Weitz, D.; Poulin, P. Structure of adhesive emulsions. *Langmuir* **1993**, *9*, 3352−3356.

(47) Dickhout, J. M.; Moreno, J.; Biesheuvel, P. M.; Boels, L.; Lammertink, R. G. H.; de Vos, W. M. Produced water treatment by membranes: A review from a colloidal perspective. *J. Colloid Interface Sci.* **2017**, *487*, 523−534.

(48) Ulbricht, M. Advanced functional polymer membranes. *Polymer* **2006**, *47*, 2217−2262.